

LETTER TO THE EDITOR

# X-ray emission from dense plasma in CTTs: Hydrodynamic modeling of the accretion shock

G. G. Sacco<sup>1,2</sup>, C. Argiroffi<sup>3,2</sup>, S. Orlando<sup>2,1</sup>, A. Maggio<sup>2</sup>, G. Peres<sup>3,2,1</sup>, and F. Reale<sup>3,2,1</sup>

<sup>1</sup> Consorzio COMETA, Via S. Sofia, 64, 95123, Catania, Italy  
e-mail: sacco@astropa.inaf.it

<sup>2</sup> INAF-Osservatorio Astronomico di Palermo, Piazza del Parlamento, 1, 90134, Palermo, Italy

<sup>3</sup> DSFA-Università degli Studi di Palermo, Piazza del Parlamento, 1, 90134, Palermo, Italy

Received 5 August 2008/Accepted 1 October 2008

## ABSTRACT

**Context.** High spectral resolution X-ray observations of classical T Tauri stars (CTTs) demonstrate the presence of plasma at  $T \sim 2-3 \times 10^6$  K and  $n_e \sim 10^{11}-10^{13}$  cm<sup>-3</sup>, unobserved in non-accreting stars. Stationary models suggest that this emission is due to shock-heated accreting material, but they do not allow to analyze the stability of such material and its position in the stellar atmosphere.

**Aims.** We investigate the dynamics and the stability of shock-heated accreting material in classical T Tauri stars and the role of the stellar chromosphere in determining the position and the thickness of the shocked region.

**Methods.** We perform 1-D hydrodynamic simulations of the impact of the accretion flow onto chromosphere of a CTT, including the effects of gravity, radiative losses from optically thin plasma, thermal conduction and a well tested detailed model of the stellar chromosphere. Here we present the results of a simulation based on the parameters of the CTT MP Mus.

**Results.** We find that the accretion shock generates an hot slab of material above the chromosphere with a maximum thickness of  $1.8 \times 10^9$  cm, density  $n_e \sim 10^{11}-10^{12}$  cm<sup>-3</sup>, temperature  $T \sim 3 \times 10^6$  K and uniform pressure equal to the ram pressure of the accretion flow ( $\sim 450$  dyn cm<sup>-2</sup>). The base of the shocked region penetrates the chromosphere and stays where the ram pressure is equal to the thermal pressure. The system evolves with quasi-periodic instabilities of the material in the slab leading to cyclic disappearance and re-formation of the slab. For an accretion rate of  $\sim 10^{-10} M_{\odot}$  yr<sup>-1</sup>, the shocked region emits a time-averaged X-ray luminosity  $L_X \approx 7 \times 10^{29}$  erg s<sup>-1</sup>, which is comparable to the X-ray luminosity observed in CTTs of the same mass. Furthermore, the X-ray spectrum synthesized from the simulation matches in detail all the main features of the O VIII and O VII lines of the star MP Mus.

**Key words.** X-rays:stars - stars: formation - accretion - hydrodynamics - shock waves - methods:numerical

## 1. Introduction

Pre-main sequence stars are strong X-ray emitters, with X-ray luminosity up to  $10^3$  times the solar value ( $L_X \sim 10^{27}$  erg s<sup>-1</sup>). Similarly to main-sequence stars, the X-rays are likely produced by low density ( $n_e \sim 10^{10}$  cm<sup>-3</sup>) plasma enclosed in coronal loop structures and heated at temperature  $T \sim 10^6 - 10^7$  K (Feigelson & Montmerle 1999). During the last five years, high resolution ( $R \sim 600$ ) X-ray observations of some classical T Tauri stars (CTTs) (TW Hya, BP Tau, V4046 Sgr, MP Mus and RU Lupi) have shown the presence of X-ray plasma at  $T \sim 2 - 3 \times 10^6$  K and denser than  $10^{11}$  cm<sup>-3</sup> (Kastner et al. 2002; Schmitt et al. 2005; Günther et al. 2006; Argiroffi et al. 2007; Robrade & Schmitt 2007), which suggests an origin different from the coronal one.

Calvet & Gullbring (1998) and Lamzin (1998) proposed that, X-ray emission from CTTs could also be produced by the accreting material. In fact the material heated by the accretion shock at the base of the accretion column could reach a temperature  $T \sim 10^6$  K. Starting from the hypothesis of the presence of a stationary strong accretion shock and solving the conservation laws for the shock-heated region, Günther et al. (2007) have quantitatively demonstrated that the accretion shock model well explains some non coronal features of the X-ray observations of TW Hya. However, these models are based on several

approximations and do not include a detailed model of the stellar atmosphere, which indeed determines the shock position and could influence the profile of pressure and density and, therefore, the thickness of the shocked region. They assume stationary conditions, but different studies proved the existence of thermal instabilities in presence of an accreting flow impacting onto a stellar surface (Langer et al. 1981; Chevalier & Imamura 1982; Koldoba et al. 2008). Considering that the physical structure of the shock-heated region and of its temporal evolution determines the fraction of the accreting energy re-emitted in the X-ray band and its spectral behavior, further investigations on the issues discussed above are required to understand better the X-ray emission from shock-heated plasma, to check their observability and, then, to derive the physical properties of the accretion process from high resolution X-ray observations.

Here we address these issues with the aid of a time-dependent hydrodynamic numerical model describing the impact of an accretion stream onto the chromosphere of a CTT. As a first application, we compared the X-ray spectra of the CTT MP Mus (Argiroffi et al. 2007) with those synthesized from the results of a simulation tuned on this star.

## 2. The model

We assume that the accretion occurs along a magnetic flux tube linking the circumstellar disk to the star. We consider the flux tube analogous to closed coronal loops observed on the Sun; therefore, as done for standard coronal loop models (e.g. Peres et al. 1982; Betta et al. 1997), we assume that the plasma moves and transports energy exclusively along the magnetic field lines. This hypothesis is supported by the low value of the plasma parameter  $\beta = P/(B^2/8\pi) \sim 10^{-2}$ , where  $P \sim 4 \times 10^2$  dyn/cm<sup>2</sup> is the expected post-shock zone pressure and  $B \sim 10^3$  G is the typical magnetic field at the surface of a CTTS (Johns-Krull 2007). Note that plasma density and velocity are expected to vary across the section of an accretion stream (e.g. Romanova et al. 2003). However, in the case of  $\beta \ll 1$ , the stream can be considered as a bundle of “elementary” streams, each characterized by different values of density and velocity. Our 1-D model describes one of these elementary streams. We limit our analysis to the impact of the accretion stream onto the chromosphere and consider the portion of the flux tube close to the star. We assume the magnetic field lines perpendicular to the stellar surface and a plane parallel geometry.

The impact of the accretion stream onto the chromosphere is modeled by numerically solving the time-dependent fluid equations of mass, momentum, and energy conservation, taking into account the gravity stratification, the thermal conduction (including the effects of heat flux saturation) and the radiative losses from an optically thin plasma:

$$\frac{\partial \rho}{\partial t} + \frac{\partial \rho v}{\partial s} = 0, \quad (1)$$

$$\frac{\partial \rho v}{\partial t} + \frac{\partial (P + \rho v^2)}{\partial s} = \rho g, \quad (2)$$

$$\frac{\partial \rho E}{\partial t} + \frac{\partial (\rho E + P)v}{\partial s} = \rho v g + E_H - \frac{\partial q}{\partial s} - n_e n_H \Lambda(T), \quad (3)$$

$$\epsilon = \frac{P}{\rho(\gamma - 1)}, \quad P = (1 + \beta(\rho, T)) \frac{\rho k_b T}{m_A}$$

where  $t$  is the time,  $s$  the coordinate along the magnetic field lines,  $\rho$  the mass density,  $v$  the plasma velocity,  $P$  the thermal pressure,  $g(s)$  the gravity,  $T$  the plasma temperature,  $E = \epsilon + v^2/2$  the total gas energy per unit mass,  $\epsilon$  the internal energy per unit mass,  $q$  the heat flux in the formulation of Spitzer (1962) corrected for the effect of flux saturation (Cowie & McKee 1977),  $n_e$  and  $n_H$  are the electron number density and hydrogen number density, respectively,  $\Lambda(T)$  is the radiative losses per unit emission measure,  $\beta(\rho, T)$  the fractional ionization ( $n_e/n_H$ ) derived from the modified Saha equation (see Brown 1973 for the solar chromosphere condition),  $\gamma = 5/3$  is the ratio between the specific heats,  $m_A = 2.14 \times 10^{-24}$  g is the average atomic mass (assuming heavy elements abundances 0.5 the solar values; Anders & Grevesse 1989), and  $E_H$  is a parametrized chromospheric heating function ( $E_H = 0$  for  $T > 8 \times 10^3$  K) defined, as in Peres et al. (1982), to keep the unperturbed chromosphere in stable equilibrium. The radiative losses per unit emission measure are derived by the PINTofALE spectral code (Kashyap & Drake 2000) with the APED V1.3 atomic line database (Smith et al. 2001), and assuming heavy elements abundances 0.5 the solar values (Anders & Grevesse 1989), as obtained from X-ray observations of CTTSs by Telleschi et al. (2007). The equations are solved numerically using the FLASH

code (Fryxell et al. 2000), an adaptive mesh refinement multi-physics code for astrophysical plasmas. The code has been extended with additional computational modules to handle the radiative losses, the thermal conduction, and the evolution of fractional ionization ( $n_e/n_H$ ).

The computational domain extends over a range  $D = 4.34 \times 10^9$  cm above the stellar surface. We allow for 5 levels of refinement in the adaptive mesh algorithm of FLASH (PARAMESH; MacNeice et al. 2000), with resolution increasing twice at each refinement level:  $\Delta s_{max} = 2.1 \times 10^6$  cm at the coarsest resolution, and  $\Delta s_{min} = 1.3 \times 10^5$  cm at the finest level, which would correspond to a uniform mesh of  $\sim 30000$  grid points. We analyzed the effect of spatial resolution on our results by considering two additional simulations which use a setup identical to the one discussed here, but with either 4 or 6 levels of refinement. We found that the adopted resolution is the best compromise between accuracy and computational cost and that the system evolution is well described in its detail.

The simulation presented here covers a time interval of about 2000 s. We used the accretion parameters (velocity and density) derived by Argiroffi et al. (2007) to match the soft X-ray emission of MP Mus. We calculated the gravity considering the star mass  $M = 1.2M_\odot$  and the star radius  $R = 1.3R_\odot$  used by Argiroffi et al. (2007).

The external part of the initial configuration, extending from  $2.75 \times 10^8$  to  $4 \times 10^9$  cm, consists of an accretion stream constant in density ( $n_e = 10^{11}$  cm<sup>-3</sup>), temperature ( $T = 10^3$  K) and velocity ( $v = 450$  km/s). The inner part of the initial configuration consists of a static chromosphere. We reproduce the pressure gradient of a young stellar chromosphere by considering the temperature profiles prescribed by Vernazza et al. (1973) solar chromosphere models scaled in order to match a pressure of  $\sim 7 \times 10^4$  dyn cm<sup>-2</sup> at the base of the chromosphere. As boundary conditions we consider fixed values both at the top ( $n_{acc} = 10^{11}$  cm<sup>-3</sup>,  $T_{acc} = 10^3$  K,  $v_{acc} = 450$  km/s) and at the base ( $n_{chr} = 10^{17}$  cm<sup>-3</sup>,  $T_{chr} = 4.44 \times 10^3$  K,  $v_{chr} = 0.0$  km/s) of the computational domain. In principle these boundary conditions lead to accumulation of matter at the base of the chromosphere. However, we have estimated that this effect becomes significant on a timescale 200 times longer than that explored by our simulation. In fact, we checked that, for  $s < 10^8$  cm, the chromosphere remains virtually unperturbed (with variations of mass density below 1%) during the timescale considered. Note also that we neglect the heating of the chromosphere (in particular, at the lower boundary) due to the X-ray emission originating from hot plasma. In the case of MP Mus (effective temperature  $T_{eff} \sim 5000$  K), this approximation is justified by the low ratio between the energy flux coming from the accretion flow and from the photospheric emission,  $(\rho_{acc} v_{acc}^3)/(4\sigma T_{eff}^4) \approx 0.1$ , where  $\sigma$  is the Stefan-Boltzmann constant. The stability of the chromosphere was tested by dedicated simulations longer than 100 ks, some of which considering also strong transient heating.

## 3. Results

The impact of the accretion stream onto the stellar chromosphere leads to the formation of transmitted (into the chromosphere) and reverse (into the accretion column) shocks. The latter propagates through the accretion column building up an hot slab. As pointed out by Argiroffi et al. (2007), in the strong shock limit (Zel'Dovich & Raizer 1967), the expected temperature of the slab is  $\sim (3/16)(\mu m_H/k_b)v_{acc}^2 \approx 3 \times 10^6$  K and, since it is subject to the radiative cooling, the expected maximum thickness is  $\sim v_{ps}\tau_{rad}$ , where  $v_{ps} = v_{acc}/4 \approx 100$  km s<sup>-1</sup> is the post-shock

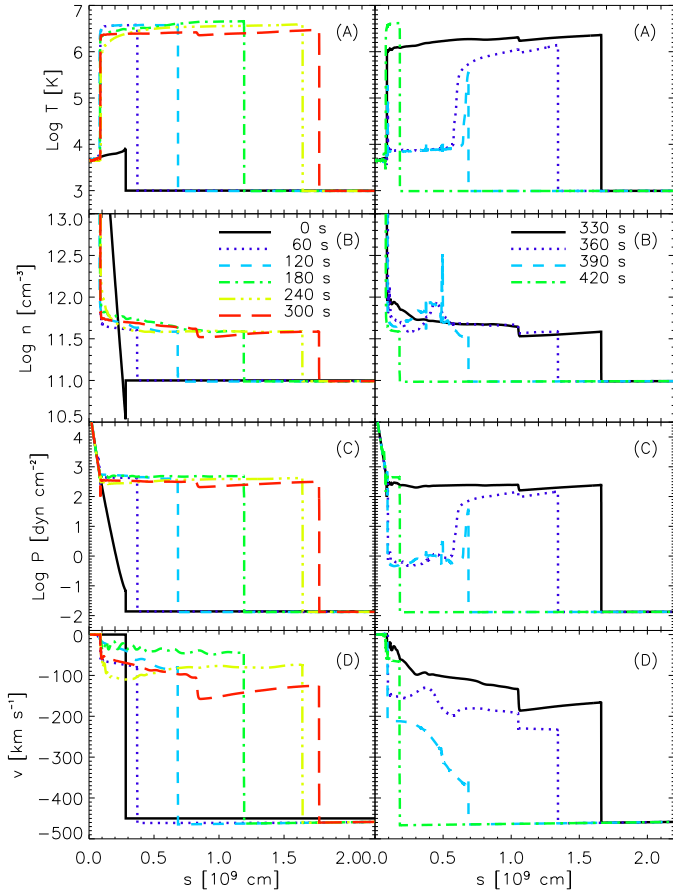


**Fig. 1.** Evolution of plasma temperature (A), density (B), pressure (C), and velocity (D) distributions along the flux tube from the chromosphere to the unperturbed accretion stream, sampled every 60 s from 0 to 300 s (left panels) and every 30 s from 330 to 420 s (right panels). The figure shows the inner portion of the spatial domain, including the chromosphere and the hot slab.

plasma velocity in the slab and  $\tau_{rad}$  is the cooling time for the shocked gas defined as

$$\tau_{rad} = \frac{1}{\gamma - 1} \frac{P}{n_e n_H \Lambda(T)} \sim 6.7 \times 10^3 \frac{T^{3/2}}{n_e}, \quad (4)$$

where, for temperatures characteristic of the slab ( $T \approx 10^5 - 10^7$  K), we approximated the cooling function as  $\Lambda(T) \approx 6.0 \times 10^{-20} T^{-1/2}$  erg s $^{-1}$  cm $^3$ . For the typical values of  $T$  and  $n_e$  of the hot slab ( $T \approx 3 \times 10^6$  K and  $n_e = 4 n_{acc} \sim 4 \times 10^{11}$  cm $^{-3}$ ),  $\tau_{rad} \approx 90$  s and the thickness of the slab is expected to be  $D_{slab} \approx 10^9$  cm. Note that deviations from equilibrium of ionization may be present beyond the shock surface due to the rapid growth of temperature (e.g. Lamzin 1998). However, these deviations are expected within a distance  $d_{NEI} \lesssim v_{ps} \tau_{eq} \sim 10^7$  cm from the shock, where  $\tau_{eq}$ , the ionization equilibrium timescale, has been estimated for the characteristic density and temperature of the slab. Being  $d_{NEI} \ll D_{slab}$ , the non-equilibrium ionization effects are not relevant for the evolution of the hot slab.

The evolution of temperature, density, pressure and velocity during the first part of our simulation is shown in Fig. 1. During the first 300 s of evolution, the reverse shock gradually heats up the accretion column at  $T \sim 3 \times 10^6$  K and the inflow piles up material creating a hot slab with density  $n_e = 3 - 7 \times 10^{11}$  cm $^{-3}$

and constant pressure equal to the accretion flow ram pressure  $P_{ram} = \rho_{acc} v_{acc}^2 = 450$  dyn cm $^{-2}$  (see left panels of Fig. 1). The base of the shocked region initially penetrates the chromosphere and comes at rest where the ram pressure is equal to the thermal pressure. The ram pressure, therefore, determines the position of the slab inside the chromosphere, while the chromosphere below the shock region remains virtually unperturbed. Due to pile up of material at the base of the shocked column, the radiative losses gradually increase there. At the end of this phase, the extension of the hot slab is  $\approx 1.8 \times 10^9$  cm.

In the subsequent phase of evolution, the strong radiative cooling of the high density plasma accumulated at the base of the hot slab triggers thermal instabilities there (Field 1965; see right panels of Fig. 1): plasma temperature and pressure decrease by more than two orders of magnitude in few seconds, leading to the collapse of the upper layers of the accretion column. As a consequence, the residual hot slab falls down and the reverse shock moves downward to the chromosphere. The additional compression due to the collapse leads to the further increase of plasma density and radiative cooling at the base of the hot slab which gradually cools down in  $\sim 100$  s.

After the accretion column is completely cooled, a new hot slab is generated (see the dashed-dotted lines in the right panels of Fig. 1) and the system starts a quasi-periodic evolution with alternating heating and cooling phases lasting  $\sim 400$  s linked to the up and down displacement of the reverse shock. Our simulation tracks the system evolution for 5 periods without significant differences among them. Therefore, we presume that the results can be extended to longer time intervals. Note that the period of the fluctuation depends on the parameters of the inflow and partially of the chromosphere. The assumption of steady flow is appropriate over the limited time explored. The whole issue should be revisited for simulations covering timescales comparable to those of changes due to stellar rotation, magnetic field evolution, etc. .

Note that Langer et al. (1981) have found periodic variations of the accretion shock position and, therefore, of the thickness of the hot slab in the context of compact objects. As in our case, the cycle consists of time intervals when the shock moves upward and the gas accumulates behind it and phases during which the shock moves downward as the hot gas cools radiatively. In the context of CTTs, Koldoba et al. (2008) found oscillations of the accretion shock position with periods  $\sim 0.02 - 0.2$ , due to the same mechanism described here. These short periods are mainly due to the set of values of accretion flow parameters (velocity and density) and heavy elements abundances adopted by these authors. In addition, our model includes the effects of thermal conduction (important in the energy budget) and the stellar chromosphere (which determines the shock position).

We checked the observability of the X-ray emission produced by the shock-heated material by synthesizing the spectrum in the energy range [0.5 – 8.0] KeV from the simulation results, and by calculating the time-average luminosity over the time interval covered by the simulation<sup>1</sup> Since our model is 1-D, we have to assume the flux tube cross section. Considering the velocity of the accretion stream  $v = 450$  km s $^{-1}$ , its density  $n_e = 10^{11}$  cm $^{-3}$  and an accretion rate  $\sim 10^{-10} M_{\odot}$  yr $^{-1}$ , the accretion stream cross section is  $\sim 6.5 \times 10^{20}$  cm $^2$ . Using this cross section, we obtain an X-ray luminosity varying from  $\sim 8.4 \times 10^{21}$  to  $\sim 1.6 \times 10^{30}$  erg s $^{-1}$  with a time-average value of

<sup>1</sup> High resolution X-ray spectra of CTTs are gathered with exposure times of  $\sim 10 - 100$  ks, i.e. much larger than the time interval covered by our simulation.

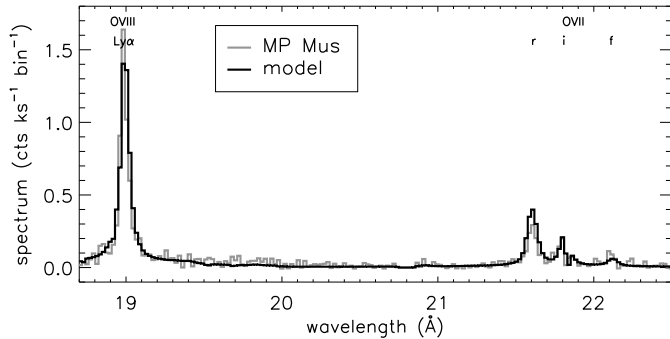


**Fig. 2.** Observed X-ray spectrum of the star MP Mus (gray line) with the synthetic spectrum derived from the simulation (black line).

$L_X = 7.2 \times 10^{29} \text{ erg s}^{-1}$ . Since this value is comparable with the typical overall luminosity observed in the young T Tauri stars of the same mass (Preibisch et al. 2005), our model shows that the shock-heated material can contribute to the X-ray emission of the CTTSs.

In Fig. 2, we compare the X-ray spectrum synthesized from the simulation (averaged over the time interval covered by the simulation) with the spectrum of the star MP Mus observed with the Reflection Grating Spectrometers (RGS) on board the XMM-Newton satellite (Argiroffi et al. 2007). The synthesis of the X-ray spectrum takes into account the instrumental response of XMM-RGS and the interstellar absorption ( $N_H = 5 \times 10^{20} \text{ cm}^{-2}$ ) derived from the observations, and assumes the emitting source at the same distance of MP Mus (86 pc). We also assumed that the time-average X-ray luminosity produced by the shock-heated slab in the 18 – 23 Å wavelength range is equal to the observed MP Mus luminosity in the same range. With the above assumptions, it turns out that the accretion rate is  $\sim 7.7 \times 10^{-11} M_\odot \text{ yr}^{-1}$  and the accretion stream cross section is  $\sim 5 \times 10^{20} \text{ cm}^2$  (i.e. a surface filling factor of about 0.5%). These values are in agreement with those ( $\sim 5 \times 10^{-11} M_\odot \text{ yr}^{-1}$  and  $\sim 3 \times 10^{20} \text{ cm}^2$ ) derived by Argiroffi et al. (2007) from the analysis of the observations.

Figure 2 shows O VIII Ly $\alpha$  and the O VII triplet. The ratio between the O VIII Ly $\alpha$  and the O VII resonance line is a tracer of plasma temperature and the ratio between the O VII forbidden and intercombination lines is a tracer of plasma density. The good agreement between the observed and the synthetic line profiles demonstrates that our model is able to explain the origin of the whole dense X-ray plasma observed in CTTSs. Furthermore, our hypothesis on heavy elements abundances is supported by the agreement of the ratio between lines and continuum intensity.

## 4. Conclusions

We model the impact of an accretion flow on the chromosphere of a young T Tauri star. Our main results are:

- the impact is able to build up a slab of accreting plasma with density  $n_e \sim 5 \times 10^{11} \text{ cm}^{-3}$  and temperature  $T \sim 3 \times 10^6 \text{ K}$ ;
- the pressure along the slab is uniform and equal to the ram pressure of the accretion shock; therefore, the slab is rooted down in the chromosphere where the thermal pressure is equal to the ram pressure;

- the thickness of the slab grows until it reaches  $\sim 1.8 \times 10^9 \text{ cm}$ , when it undergoes a thermal collapse due to the enhancement of density and, therefore, of radiative losses at its base;
- the system oscillates quasi-periodically between the formation of an hot slab and its thermal collapse by thermal instability;
- according to our model, an accretion rate of  $\sim 10^{-10} M_\odot \text{ yr}^{-1}$  is enough to produce an X-ray luminosity varying between  $\sim 8.4 \times 10^{21}$  and  $1.6 \times 10^{30} \text{ erg s}^{-1}$ , with a time-average value of  $L_X \sim 7 \times 10^{29} \text{ erg s}^{-1}$ , which is comparable to the overall X-ray luminosity observed in the CTTSs of the same mass;
- our model is able to explain in detail the observed X-ray spectrum of the star MP Mus (Argiroffi et al. 2007).

A large set of simulations, exploring the domain of the physical parameters of the system, will be studied in a future paper.

*Acknowledgements.* We thank Jeremy Drake for useful discussions. This work was supported in part by the Italian Ministry of University and Research (MIUR) and by Istituto Nazionale di Astrofisica (INAF). The software used in this work was in part developed by the DOE-supported ASC / Alliance Center for Astrophysical Thermonuclear Flashes at the University of Chicago. This work makes use of results produced by the PI2S2 Project managed by the Consorzio COMETA, a project co-funded by the Italian Ministry of University and Research (MIUR) within the Piano Operativo Nazionale “Ricerca Scientifica, Sviluppo Tecnologico, Alta Formazione” (PON 2000-2006). More information is available at <http://www.pi2s2.it> and <http://www.consorzio-cometa.it>.

## References

- Anders, E. & Grevesse, N. 1989, *Geochim. Cosmochim. Acta*, 53, 197
- Argiroffi, C., Maggio, A., & Peres, G. 2007, *A&A*, 465, L5
- Betta, R., Peres, G., Reale, F., & Serio, S. 1997, *A&AS*, 122, 585
- Brown, J. C. 1973, *Sol. Phys.*, 29, 421
- Calvet, N. & Gullbring, E. 1998, *ApJ*, 509, 802
- Chevalier, R. A. & Imamura, J. N. 1982, *ApJ*, 261, 543
- Cowie, L. L. & McKee, C. F. 1977, *ApJ*, 211, 135
- Feigelson, E. D. & Montmerle, T. 1999, *ARA&A*, 37, 363
- Field, G. B. 1965, *ApJ*, 142, 531
- Fryxell, B., Olson, K., Ricker, P., et al. 2000, *ApJS*, 131, 273
- Günther, H. M., Liefke, C., Schmitt, J. H. M. M., Robrade, J., & Ness, J.-U. 2006, *A&A*, 459, L29
- Günther, H. M., Schmitt, J. H. M. M., Robrade, J., & Liefke, C. 2007, *A&A*, 466, 1111
- Johns-Krull, C. M. 2007, *ApJ*, 664, 975
- Kashyap, V. & Drake, J. J. 2000, *Bulletin of the Astronomical Society of India*, 28, 475
- Kastner, J. H., Huenemoerder, D. P., Schulz, N. S., Canizares, C. R., & Weintraub, D. A. 2002, *ApJ*, 567, 434
- Koldoba, A. V., Ustyugova, G. V., Romanova, M. M., & Lovelace, R. V. E. 2008, *MNRAS*, 388, 357
- Lamzin, S. A. 1998, *Astronomy Reports*, 42, 322
- Langer, S. H., Chanmugam, G., & Shaviv, G. 1981, *ApJ*, 245, L23
- MacNeice, P., Olson, K. M., Mobarrry, C., de Fainchtein, R., & Packer, C. 2000, *Computer Physics Communications*, 126, 330
- Peres, G., Serio, S., Vaiana, G. S., & Rosner, R. 1982, *ApJ*, 252, 791
- Preibisch, T., Kim, Y.-C., Favata, F., et al. 2005, *ApJS*, 160, 401
- Robrade, J. & Schmitt, J. H. M. M. 2007, *A&A*, 473, 229
- Romanova, M. M., Ustyugova, G. V., Koldoba, A. V., Wick, J. V., & Lovelace, R. V. E. 2003, *ApJ*, 595, 1009
- Schmitt, J. H. M. M., Robrade, J., Ness, J.-U., Favata, F., & Stelzer, B. 2005, *A&A*, 432, L35
- Smith, R. K., Brickhouse, N. S., Liedahl, D. A., & Raymond, J. C. 2001, *ApJ*, 556, L91
- Spitzer, L. 1962, *Physics of Fully Ionized Gases* (New York: Wiley)
- Telleschi, A., Güdel, M., Briggs, K. R., Audard, M., & Scelsi, L. 2007, *A&A*, 468, 443
- Vernazza, J. E., Avrett, E. H., & Loeser, R. 1973, *ApJ*, 184, 605
- Zel'Dovich, Y. B. & Raizer, Y. P. 1967, *Physics of shock waves and high-temperature hydrodynamic phenomena*, ed. Hayes, W. D., Probstein, R. F. (New York: Academic Press)